

Development of an Electrochemical Paper-Based Analytical Device for Trace Detection of Virus Particles

Robert B. Channon,^{†,#} Yuanyuan Yang,^{†,#} Kristen M. Feibelman,[‡] Brian J. Geiss,^{‡,¶} David S. Dandy,^{§,¶} Charles S. Henry^{*,†,§,¶}

[†] Department of Chemistry, Colorado State University, Fort Collins, CO 80523, USA

[‡] Department of Microbiology, Immunology, and Pathology, Colorado State University, Fort Collins, CO 80523, USA

[§] Department of Chemical and Biological Engineering, Colorado State University, Fort Collins, CO 80523, USA

[¶] School of Biomedical Engineering, Colorado State University, Fort Collins, CO 80523, USA

[†] RB. Channon and Y. Yang contributed equally to this work.

TABLE OF CONTENTS

S1: Electrochemical Impedance Spectroscopy

S2: Investigation of Monothiol and Dithiol Stability on Au Microwires

S3: Analysis of Scanning Electron Microscopy Images

S1: ELECTROCHEMICAL IMPEDANCE SPECTROSCOPY

To demonstrate the requirement for signal normalization, Figure S1 shows the final West Nile virus (WNV) detection in a flow electrochemical paper-based analytical device (flow-ePAD) without the normalization of equation 1 from the main text. The larger error bars and offset of the unmodified device resistance to charge transfer (R_{ct}) values highlights the requirement for normalization (see Figure 7 main text).

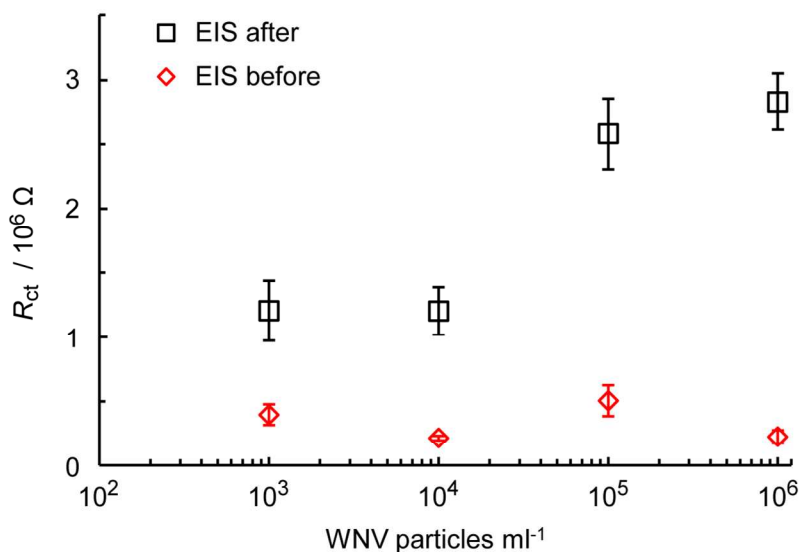


Figure S1. Resistance to charge transfer before and after addition of WNV particles (flow-ePAD, $n = 4$).

To further improve the analytical signals, the $\text{Fe}(\text{CN})_6^{3/4-}$ concentration was optimized as shown in Figure S2. 10 mM of $\text{Fe}(\text{CN})_6^{3/4-}$ (comprising 5 mM ferricyanide and 5 mM ferrocyanide) in 0.1 M PBS (pH 7) was chosen to minimize the signal and relative standard deviation of R_{ct} , and thus maximize the clarity of signal increase ($\% \Delta R_{ct}$) on target binding (see Figure 1 of main text).

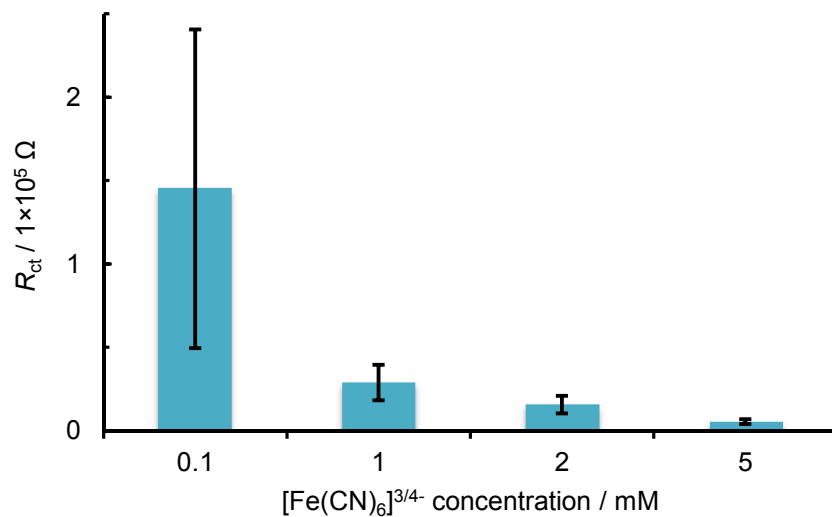


Figure S2. Resistance to charge transfer for Au microwires in different concentrations of $[\text{Fe}(\text{CN})_6]^{3/4-}$ (1:1 mixture in 0.1M KNO_3) in a static-ePAD.

S2 INVESTIGATION OF MONOTHIOL AND DITHIOL STABILITY ON AU MICROWIRES

The stability of thiol modified Au microwires were investigated through binding of a ferrocene terminated thiol ($\text{Fc}-(\text{CH})_6\text{SH}$) under different experimental conditions. After washing and fabrication into a static-ePAD, the bound ferrocene could be oxidized via cyclic voltammetry in 0.1 M KNO_3 . The resulting integrated peak area corresponds to the number of bound groups, informing on the stability of the Au-thiol self-assembled monolayer. After modification with 10 μM $\text{Fc}-(\text{CH})_6\text{SH}$ overnight under N_2 and in the dark, the modified microwires were ferrocene terminated thiol overnight, then exposed to different conditions before fabrication into a static-ePAD for cyclic voltammetry characterization of the surface. As shown in Figure S3, removal from a N_2 -infused and dark environment significantly affected the monolayer stability, resulting in a reduction in bound $\text{Fc}-(\text{CH})_6\text{SH}$ and thus smaller integrated peak area from the cyclic voltammetry. This is in line with previous investigations of thiol-gold modification stability.¹ Therefore, all devices were kept under N_2 and in the dark during modification and were fabricated into the paper-based devices as soon as possible after modification.

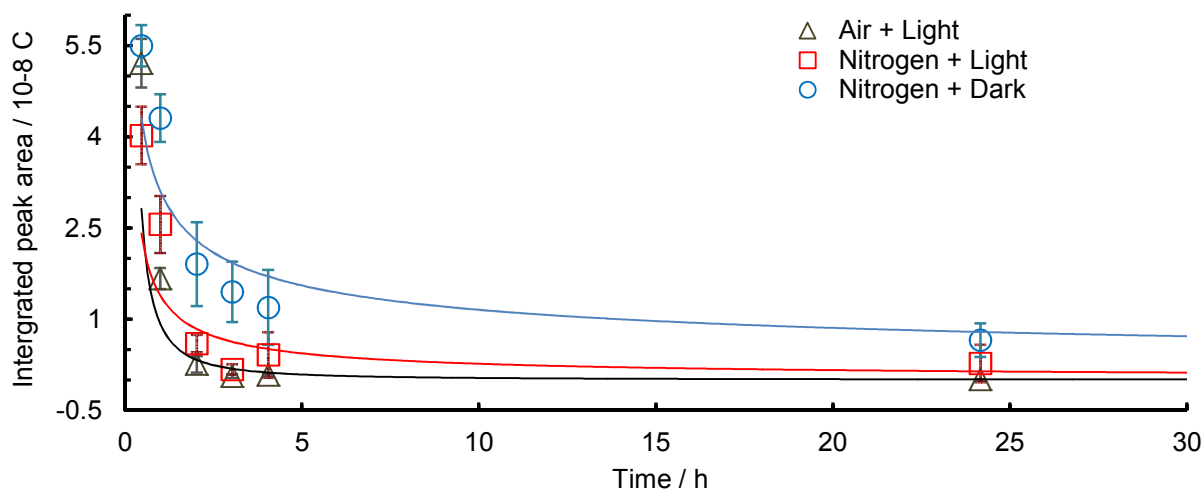


Figure S3. Stability of Au monothiol in different modification environments, studied via the decay of bound Fc-(CH)₆SH (10 μM) electro-oxidation signals through cyclic voltammetry in 0.1 M KNO₃, time represents time between modification and detection, trendlines are power fits illustrate the decay in signal (static-ePAD, n = 3).

To further assess the stability of the flow-ePADs, devices were fabricated as normal, then kept in the dark for a series of days before measurement of 1 × 10⁶ SA particles mL⁻¹ as shown in Figure S4. After a small initial increase over the first 3 days, the R_{ct} signal stabilizes over the next 12 days, indicating the flow-ePADs should be usable after long storage periods. The improved storage capacity of flow-ePADs over static-ePADs is possibly due to the effective ‘sealing’ of the wires within the flow devices, and this aspect is currently under investigation or future work.

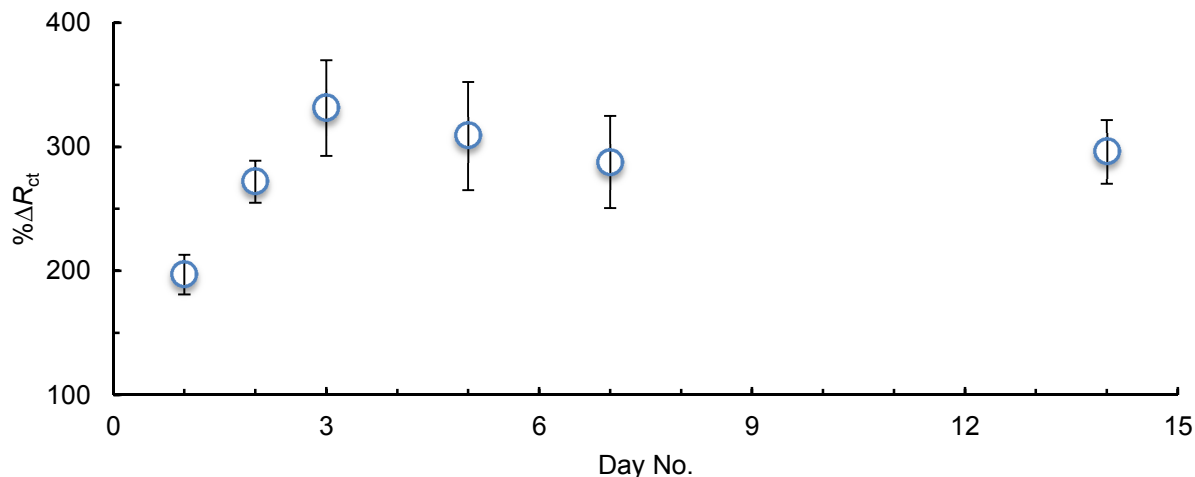


Figure S4. Stability of flow-ePAD for capturing of 1 × 10⁶ SA particles mL⁻¹ different period after fabrication (n = 3, stored in dark and air).

S3: ANALYSIS OF SCANNING ELECTRON MICROSCOPY IMAGES

Scanning electron microscopy (SEM) was carried out on 1 × 10⁶ particles mL⁻¹ SA particles with radius 100 nm, captured on a biotin-modified Au microwire electrode (25 μm radii). The SEM images were then analyzed using the following MATLAB script, based upon a circle finding function and adapted from a previous publication:²

```
I=imread('wire_3_10minsbeads_1.tif');
I2 = I(1:964,:);
imshow(I2)
[centersdark, radiidark] = imfindcircles(I2,[3
9], 'ObjectPolarity','dark','sensitivity',0.94,'edgethreshold',0.2);
viscircles(centersdark, radiidark,'color','b');
```

The density was calculated through division of the number of beads by the electrode area of each SEM image, which was adjusted to allow for the electrode curvature using the following equation:

$$Real\ surface\ area = \frac{2\pi^2rx}{\arcsin \frac{y'}{r}}$$

where x and y' are the dimensions of the SEM image as shown in Figure S3, and r is the microwire radii. The calculated particle density (2.8×10^4 SA particles mm^{-2}) and coverage (0.09%) are reasonable based on literature of aptamer modified Au electrodes.³

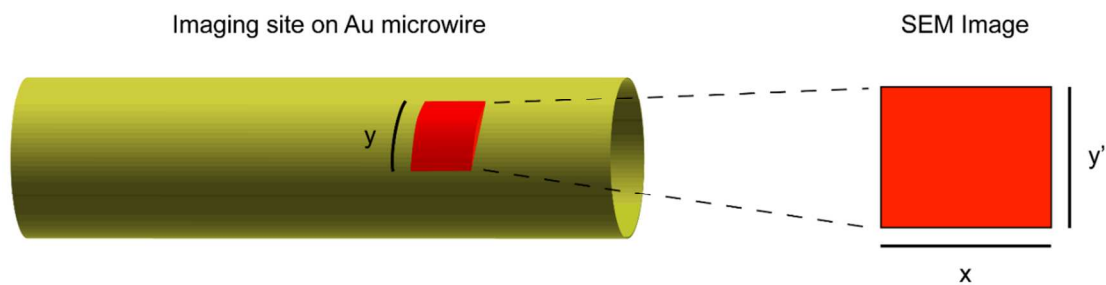


Figure S5. Calculation of the real surface area from a 2D SEM image of a microwire.

REFERENCES

- (1) Srisombat, L.; Jamison, A. C.; Lee, T. R. *Colloids Surf. A* **2011**, *390*, 1-19.
- (2) Channon, R. B.; Joseph, M. B.; Bitziou, E.; Bristow, A. W. T.; Ray, A. D.; Macpherson, J. V. *Anal. Chem.* **2015**, *87*, 10064-10071.
- (3) White, R. J.; Phares, N.; Lubin, A. A.; Xiao, Y.; Plaxco, K. W. *Langmuir* **2008**, *24*, 10513-10518.